Affiliation statement

Hao XU

Position/title: Associate Professor, PhD;

Affiliation: School of Aeronautics and Astronautics, Faculty of Vehicle Engineering and Mechanics, State Key Laboratory of Structural Analysis for Industrial Equipment, Dalian University of Technology, Dalian, 116024,China;

Mailing address: Rm 411A, No. 1 Integrated Experimental Building, Dalian University of Technology, No.2 Linggong Road, Gaoxin District, Dalian, Liaoning, China

E-Mail: xuhao@dlut.edu.cn

Qi ZHOU

Position/title: M.Phil Student;

Affiliation: School of Aeronautics and Astronautics, Faculty of Vehicle Engineering and Mechanics, State Key Laboratory of Structural Analysis for Industrial Equipment, Dalian University of Technology, Dalian, 116024,China;

Mailing address: Rm 218, Experimental Building of Aeronautics and Astronautics, Dalian University of Technology, No.2 Linggong Road, Gaoxin District, Dalian, Liaoning, China

E-Mail: zhouqi1993@dlut.edu.cn

Maosen CAO

Position/title: Professor, PhD;

Affiliation: Department of Engineering Mechanics, Hohai University, Nanjing, 210098, People's Republic of China;

Mailing address: Rm 808, Le Xue Building, Hohai University, No.8 Fo Cheng Xi Road, Jiangning District, Nanjing, Jiangsu, China

E-Mail: cmszhy@hhu.edu.cn

Zhongqing SU

Position/title: Professor, PhD;

Affiliation: Department of Mechanical Engineering, The Hong Kong Polytechnic University, Kowloon, Hong Kong SAR;

Mailing address: EF 605, The Hong Kong Polytechnic University, Kowloon, Hong Kong SAR

E-Mail: zhongqing.su@polyu.edu.hk

Zhanjun WU

Position/title: Professor, PhD;

Affiliation: School of Aeronautics and Astronautics, Faculty of Vehicle Engineering and Mechanics, State Key Laboratory of Structural Analysis for Industrial Equipment, Dalian University of Technology, Dalian, 116024,China;

Mailing address: Rm 410B, No. 1 Integrated Experimental Building, Dalian University of Technology, No.2 Linggong Road, Gaoxin District, Dalian, Liaoning, China

E-Mail: wuzhj@dlut.edu.cn

A Dynamic Equilibrium-based Damage Identification Method Free of Structural Baseline Parameters: Experimental Validation in a Two-dimensional Plane Structure

Hao XU[1], Qi ZHOU[1], Maosen CAO[2], Zhongqing SU[3] and Zhanjun WU[1†]

[1]School of Aeronautics and Astronautics, Faculty of Vehicle Engineering and Mechanics, State Key Laboratory of Structural Analysis for Industrial Equipment, Dalian University of Technology, Dalian, 116024,China

[2] Department of Engineering Mechanics, Hohai University, Nanjing, 210098, People's Republic of China

[3] Department of Mechanical Engineering, The Hong Kong Polytechnic University, Kowloon, Hong Kong SAR

Submitted to *Journal of Aerospace Engineering*

(Resubmitted on Feb. 2, 2018)

[†] To whom correspondence should be addressed
Email: wuzhj@dlut.edu.cn (Prof. Zhanjun WU, Ph.D.)

Abstract

A damage identification method named "pseudo-excitation" (PE) approach was established previously, the principle of which resides on local examination of perturbation of structural dynamic equilibrium conditions. While showing significant sensitivity to structural damage with small sizes, the approach exhibited high vulnerability to measurement noise due to the involvement of high order derivatives of the vibration displacements in the expression of the damage index. On the other hand, several baseline parameters, for example, Young's Modulus and Density, are of necessity for the implementation of the approach, considered as a factor that limits the practical application of the approach. A "weak" formulation of the PE approach was established to circumvent the interference from measurement noise. However, the weak formulation of two-dimensional (2D) structural component has not been developed, and the reliance of the weak formulation on baseline parameters remains an issue unsolved. In this paper, the 2D weak formulation of the PE approach was proposed by introducing a weighting function in terms of 2D Gauss function. Through an integration operation, the selected weighting function was shown able of significantly highlighting the feature of structural damage and largely suppressing noise influence. Furthermore, a statistical strategy was developed to estimate the values of baseline parameters inversely, which signifies the elimination of the dependence of PE approach on pre-obtained baseline parameters. As a proof-of-concept investigation, multi-damage in a plane structure consisting of both beam and plate components were identified by using the modified damage identification method. And a hybrid data fusion algorithm was then used to enhance the accuracy of damage detection, revealing not only the locations, but also the sizes of damaged zones.

Keywords**:** damage identification, dynamic equilibrium, vibration, statistical estimation, measurement noise

Introduction

In recent decades, structural health monitoring (SHM) techniques have been largely developed with the aim of continuous and automated structural damage evaluation. The majority of existing SHM techniques were established based on characteristics either of guided wave propagation or structural vibration. The guided-wave-based methods (using for instance Lamb waves (Gao et al. 2014; Gao et al. 2016; Ihn and Chang 2008; Liu et al. 2016; Ostachowicz et al. 2009; Su et al. 2006; Wu et al. 2015; Zhao et al. 2007;)) possess high sensitivity to structural damage with significantly small size. The accuracy of the methods, however, could be largely limited due to the complex geometries or boundary conditions of the structure under inspection. Moreover, active excitation is of necessity for the generation of wave signals, involving relatively complex experimental configurations. The vibration-based methods (Farrar et al. 2001; Fan and Qiao 2011; Joshuva and Sugunaran 2017), on the other hand, can be implemented based on the changes in a number of different vibration signatures, for example, eigen-frequencies (Guo and Li 2011; Lee and Chung 2000; Salawu 1997), mode shape or modal curvature (Cao et al. 2013; Kim et al. 2003; Pandey et al. 1991), electro-mechanical impedance (Giurgiutiu and Rogers 1998;), flexibility matrix (Aoki and Byon 2001; Pandey and Biswas 1994; Siddesha and Manjunath 2017; Yan and Golinval 2005) and damping properties (Kawiecki 2001). In engineering applications, these vibration signatures are convenient to obtain under structural operational state, without any necessity of active excitation. The effectiveness of traditional guided-wave- or vibration-based methods, however, largely depend on the obtainment of benchmark structures and baseline signals that need to be established numerically or experimentally, which considered as a drawback that limits the efficiency and accuracy of damage identification. To circumvent such a limitation, a new method relying on the examination of local perturbation of structural dynamic equilibrium, named Pseudo-excitation (PE) approach, was proposed by the authors

(Xu et al. 2011; Xu et al. 2013);. Specifically, the damage index of the PE approach was derived based on the equation of motion for different types of structural components, e.g., beam, plate or shell components. And the locations and sizes of the damaged zones can be revealed according to the singularities of the damage indices, which correspond to perturbed dynamic equilibrium conditions. The PE approach was proven capable of detecting damage with satisfactory sensitivity, without any prior knowledge from the baseline signals or benchmark structures. However, the method suffers from interference of measurement noise due to the involvement of high-order derivatives of structural vibration displacements in the expressions of the damage indices. On the other hand, some baseline parameters (Young's Modulus, density, etc.) of the inspected structure still need to be obtained before the implementation of the method, deemed as an obstacle that limit the effectiveness and efficiency of the original PE approach.

The "weak" formulation of the PE index for one-dimensional (1D) beam component was proposed (Xu et al. 2015a), where different expanded forms can be established to include the measurement of different mechanical quantities, e.g., vibration displacement and structural surface strains. The main task of the weak formulation is to reduce the influence of measurement noise on the accuracy of damage identification. Moreover, by assuming point-wise satisfaction of dynamic equilibrium along a beam structure, the PE approach shows potential of damage identification without any dependence on structural baseline parameters (Xu et al. 2015b). In this study, the application of the modified PE approach was extended to characterize multi-damage in 2D structures. The weak formulation of 2D damage index was established, relying on which damage features can be largely highlighted, benefiting from the effectiveness of noise reduction. In addition, the assumption of point-wise satisfaction of dynamic equilibrium was made along 2D plate structure. Thus damage can be detected without baseline parameters. Moreover, some baseline parameters of the inspected structure can be inversely estimated in a statistical manner, showing promising potential in engineering practices. As a proof-of-concept investigation, multi-damage in a plane structure, containing both beam and plate components, were identified experimentally using the proposed method. A hybrid data fusion algorithm was then used to enhance the accuracy of damage detection, revealing not only the locations, but also the sizes of damaged zones.

Modified PE Approach Based on "Weak" Formulation

For a damaged plate structure as shown in Fig. 1, the 2D damage index of the original PE approach can be expressed as (Xu et al. 2013):

$$\mathrm{DI}(x,y) = D\Phi(x,y) - \rho h\omega^2 w(x,y), \tag{1a}$$

where

$$\Phi(x,y) = \frac{\partial^4 w(x,y)}{\partial x^4} + 2\frac{\partial^4 w(x,y)}{\partial x^2 \partial y^2} + \frac{\partial^4 w(x,y)}{\partial y^4} \quad . \tag{1b}$$

In the above equations, $w(x,y)$ is the vibration displacements; D is the bending stiffness equal to $Eh^3/12(1-\nu^2)$, where E, ρ, ν, h and ω are the Young's Modulus, density, Poisson's ratio, thickness and angular vibration frequency of the plate, respectively. In numerical computation, Eq. (1b) can be expressed in a discrete form by using a finite difference scheme (Xu et al. 2013). Equation (1a) was derived based on the equation of motion for plate structure, indicating the local dynamic equilibrium condition of infinitesimal plate element. For an element without damage and external excitation, $\mathrm{DI}(x,y)$ in Eq. (1a) should be zero because of the satisfaction of dynamic equilibrium condition. Where damage exists, $\mathrm{DI}(x,y)$ will show drastic fluctuations in magnitudes, particularly at the boundaries of the damaged zone, due to the violation of the local equilibrium condition in Eq. (1a).

From the above equations, it can be seen that a variety of baseline parameters, including the Young's modulus and different parameters associated with structural geometries, should be obtained for the construction of Eq. (1a). With the purpose of eliminating the reliance of the PE approach on structural baseline parameters, the damage index in Eq. (1a) was modified to be

$$\Im(x,y)=\Phi(x,y)-\lambda^{*}w(x,y)\,, \tag{2a}$$

where

$$\Im(x,y)=\frac{\mathrm{DI}(x,y)}{D} \quad \text{and} \quad \lambda^{*}=\frac{\rho h\omega^{2}}{D}\,. \tag{2b}$$

It can be seen that all baseline parameters have been included in the expression of λ^{*}. The value of λ^{*} can be estimated in a statistical manner, which will be introduced in the following section.

The 1D weak formulation of PE approach was developed for the purpose of noise reduction and enabling the flexibility of measuring multiple types of mechanical quantities for damage detection, e.g., vibration displacement and surface strains (Xu et al. 2015a). In this study, the weak formulation for 2D PE approach was derived based on Eq. (2a), expressed as

$$\bar{\Im}(x,y)=\int_{\Xi}\Im(x,y)\eta(x,y)\mathrm{dxdy}\,. \tag{3a}$$

Substituting Eq. (2a) into (3a) yields

$$\bar{\Im}(x,y)=\int_{\Xi}\Phi(x,y)\eta(x,y)\mathrm{dxdy}\text{-}\lambda^{*}\int_{\Xi}w(x,y)\eta(x,y)\mathrm{dxdy}\,. \tag{3b}$$

In the above equations $\eta(x,y)$ is a weighting function; Ξ is a 2D region within which the integration was operated. For the selection the form of $\eta(x,y)$, a main consideration is to effectively suppress the influence of measurement noise without sacrificing the signal feature subject to damage. Another important consideration is to enhance the flexibility of damage detection by enabling the measurement of multiple mechanical quantities. The latter task has been achieved in 1D case, where the weak formulation was expanded based on partial integration principle. For 2D case, the weak formulation in Eq. (3) is also possible to be expanded based on principles such as the Greens's theorem. However, relevant study is beyond the scope of this work. Therefore, the effectiveness of noise reduction is deemed as the major criteria for the selection of $\eta(x,y)$. Moreover, after the form of $\eta(x,y)$ being fixed, the size of the integration region Ξ, needs to be adjusted to obtain optimal accuracy of damage identification.

Estimation of Structural Baseline Parameters

In practical applications, structural damage is regarded as local event. Thus, along the surface of the structure of interest, most areas can be assumed to be under their intact state, which means that the value of Eq. (3b) can be assumed to be zero, i.e.,

$$\int_{\Xi} \Phi(x,y)\eta(x,y)\mathrm{dxdy}\text{-}\lambda^{*}\int_{\Xi} w(x,y)\eta(x,y)\mathrm{dxdy}=0 . \tag{4a}$$

Then λ^{*} can be derived to be

$$\lambda^{*}=\frac{\int_{\Xi}\Phi(x,y)\eta(x,y)\mathrm{dxdy}}{\int_{\Xi}w(x,y)\eta(x,y)\mathrm{dxdy}}. \tag{4b}$$

It can be seen that at the damaged zones, Eq. (4a) does not actually hold, and the calculated λ^{*} will differ from its actual value. Along the entire structural surface under inspection, however, Eq. (4a) does hold and a large number of λ^{*} values can be calculated and distribute around the actual value of λ^{*}. Thus the actual value of λ^{*} can be estimated in a statistical way, by calculating the average of all λ^{*} values along the inspected area. Furthermore, depending on the estimated λ^*, some baseline parameters can be calculated inversely according to Eq. (2b). For example, the Young's Modulus of the structure can be estimated when the geometric parameters and the vibration frequency of the plate are given.

For 1D structural components, i.e., beams, the baseline parameters can be estimated in an analogous way as presented by Eq. (4a). Since the details of deriving 1D weak formulation have been provided in (Xu et al. 2015a), only the expression for the inverse estimation of baseline parameters, developed in this study, is given as

$$\lambda^* = \frac{\int_\Xi \Phi(x)\eta(x)\mathrm{dx}}{\int_\Xi w(x)\eta(x)\mathrm{dx}}. \tag{4c}$$

Equation (4c) can be easily understood since it is a regressive form of Eq. (4b). $w(x)$ and $\eta(x)$ in Eq. (4c) are the 1D vibration displacement and weighting function; $\Phi(x)$ equals to $\mathrm{d}^4 w(x)/\mathrm{d}x^4$; Ξ represents a 1D integration region with a selected length. It should be noted that for beam components, the baseline parameters are included in λ^* according to $\lambda^* = \rho S\omega^2 / EI$, where S and I are the cross-section area and cross-sectional moment of inertia, respectively.

The implementation process of damage identification is illustrated by a flow chart as shown in Fig. 2. It should be emphasized that given the form of weighting function, the size of Ξ has a major influence on the accuracy of damage detection. A small Ξ could lead to high precision of damage detection by highlighting the local feature of damage, but probably will be associated with unacceptable noise influence because of insufficient signal averaging within Ξ. A larger Ξ could provide satisfactory noise reduction but may lead to low detection precision due to "over-smoothing" of the damage feature. Therefore, optimal detection accuracy corresponds to a balance between the detection precision and the noise reduction effect. In the following study, the relative size of Ξ are adjusted referring to the vibration wavelengths of tested structures, i.e., for 2D case, the ratio of the side length of Ξ to the vibration wavelength. Based on a data fusion algorithm, detection signals subject to different ratios are combined to provide the optimal detection results. The 2D data fusion algorithm used is

$$\overline{\Im}_{i,j\text{-hybrid}} = \overline{\Im}_{i,j\text{-arithmetic}} \cap \overline{\Im}_{i,j\text{-geometric}} \tag{5a}$$

where

$$\overline{\Im}_{i,j\text{-arithmetic}} = \frac{1}{K}\sum_{L=1}^{K}\overline{\Im}_{i,j-L}\ , \tag{5b}$$

$$\overline{\Im}_{i,j\text{-geometric}} = \sqrt[K]{\overline{\Im}_{i,j-1}\cdot\overline{\Im}_{i,j-2}\cdots\overline{\Im}_{i,j-L}\cdots\overline{\Im}_{i,j-K}}\ . \tag{5c}$$

In the above equations. $\overline{\Im}_{i,j\text{-hybrid}}$ is the damage index value at point (i,j) treated by hybrid fusion. $\overline{\Im}_{i,j\text{-arithmetic}}$ and $\overline{\Im}_{i,j\text{-geometric}}$ represent damage index treated by arithmetic and geometric fusion algorithm, respectively. K is the number of the total groups of data use for fusion, and L is the index of an individual data group.

Experimental Validation

Setup

Experimental validation was carried out to examine the reliability of the developed strategy in identifying multiple damaged zones in a plane structure containing both beam and plate components. The front and back views of the plane structure are shown in Fig 3(a) and (b), respectively. The structure was made of aluminum 6061 with a density of 2.7 kg/m^3 and a Young's modulus of 68.9 GPa. The thickness of the aluminum panel is 3 mm. The structure was fixed-supported on a testing table (NEWPORT® ST-UT2). From Fig 3(b), it can be seen that multi-damage was introduced in both the beam and the plate components.

Specifically, there are four damaged zones in the three beam components (beam I, II and III), in terms of through-width notches measuring 4 mm in length and 1.3 mm in depths. In beam III there are two damaged zones. A square damaged zone was created in the plate component, the side length and depth of which are 8 mm and 1.3 mm, respectively.

The plane structure was excited on the back side using an electro-mechanical shaker (B&K® 4809) located at the excitation point as shown in Fig. 3(b), in which the excitation point is 95 mm and 130 mm from the lower and the right boundary of the structure. A scanning Doppler laser vibrometer (Polytec®PSV-400B) was used to measure the vibration displacements of the structure within the inspection regions. As shown in Fig. 3(a), the square inspection region on the plate component is $210 \times 210\ \mathrm{mm}^2$ in size, containing 61×61 measurement points. It should be noted that the excitation point is not within the inspection region, but with a distance of 13 mm from the lower edge of the inspection region. The inspection regions on the beam components are $288\ mm$ in length. There are 73 measurement points along the central line of each beam component.

Damage Identification Results

Under an excitation frequency of 1800 Hz, the distribution of the vibration displacements of the plate component, within the 2D inspection region, is presented in Fig. 4(a). It can be calculated that the wavelength of the vibration of the plate component, defined as γ, is approximately 0.21 m. Based on the measured vibration displacements, the damaged zone in the plate component was first identified by using the original formulation of the PE approach as presented in Eq. (1a). It can be understood that to construct Eq. (1a), all baseline parameters of the structure need to be known. And it is shown in Fig. 4(b) that even using the baseline parameters, the constructed signal of the damage indices is incapable of reflecting any damage feature because of the severe interference from measurement noise, associated with the high-order derivatives of vibration displacements, i.e., $\Phi(x,y)$ in Eq. (1b). The density of the 4experimental data in Fig. 4(b) was enlarged by ten times through an interpolation algorithm before the implementation of weak formulations, aimed at improving the accuracy of damage detection.

The weak formulation of the PE approach, as shown in Eq. (3a), was then applied to identify the damage. The form of $\eta(x,y)$ in Eq. (3a) was selected according to a 2D Gauss function. The 2D Gauss function possesses a highly simple form and an explicit function in signal processing. On the one hand, the 2D Gauss function is able to highlight damage feature due to its large similarity with the signal feature associated with damage, that is, large local singularities (peak values). On the other hand, the gauss function is relatively smooth that can benefit the averaging of measurement noise within the integration region. Specifically, the general form of a 2D Gauss function is

$$\eta(x,y)=\frac{1}{\sqrt{2\pi\sigma^2}}e^{-\frac{x^2+y^2}{2\sigma^2}}\ , \tag{6}$$

where σ is the standard deviation of the Gauss function. Ξ in Eq. (3a) is set to be a square region, the side length of which is defined as d. It is fixed in the following analysis that $d=10\sigma$. The 2D Gauss function within Ξ is shown in Fig. 5, from which it can be seen that the majority of the energy of the Gauss function is included in Ξ, and at the boundaries of Ξ the values of the function vanish. The position of Ξ was then adjusted along the plate surface to scan the entire 2D inspection region, and λ^* was calculated according to Eq. (4b). λ^* distributions subject to $d/\gamma=0.3$, 0.4, 0.5 and 0.6 were calculated, and the distribution subject to $d/\gamma=0.4$ is shown as an example in Fig. 6. From the figure, it can be seen that the distribution of λ^* values is relatively smooth converging to an average value, although some significant fluctuations can be observed due to the influence from measurement noise.

Large fluctuations were deemed as outliers that distribute outside a pre-defined bandwidth (10% of the standard deviation of the entire data), and were excluded from the data set. Then λ^* was estimated as the average value of the remaining data. The λ^* values subject to different d/γ, as selected above, were further averaged leading to an estimated value of 6.80×10^6, around 10% larger than the actual value.

By using the estimated value of λ^*, $\overline{\Im}(x,y)$ was calculated according to Eq. (3b), and the distributions of $\overline{\Im}(x,y)$ along the 2D inspection region subject to different d/γ are shown in Fig. 7(a) to (d). From the figure, it can be seen that subject to a small value of d/γ (i.e., 0.3), the damage feature can be well highlighted by showing a relatively exact size of the damaged zone. However, noise influence is relatively severe, causing signal disturbances at the intact region of the plate. On the other hand, the noise can be increasingly reduced along with enlarged d/γ, and under $d/\gamma=0.6$, signal disturbances at intact region are largely suppressed. The damage size, however, is over-estimated under $d/\gamma=0.6$ because of the smoothing effect on the damage feature. An optimal detection accuracy can be found between $d/\gamma=0.4$ and 0.5, corresponding to which a balance between the detection precision and noise reduction can be achieved. The detection results associated with the four different d/γ were treated using hybrid data fusion algorithm as shown in Eq. (5a) to (5c), giving rise to the optimal detection result as shown in Fig. 8(a). It can be seen that the location and size of the square damaged zone are precisely revealed.

Finally, damage zones were identified in the beam components based on 1D weak formulation and the parameter estimation method as shown in Eq. (4c). One-dimensional Gauss function was selected as the weighting function, and the length of the 1D integration region Ξ was fixed to be 10σ (consistent with that in the 2D case), with σ being the standard deviation. According to $d/\gamma = 0.3$, 0.4, 0.5 and 0.6 (γ here is the 1D vibration wavelength of the beam components), distributions of λ^* were calculated according to Eq. (4c) and then averaged, leading to the estimated value of λ^* being 7.01×10^6, which is 5% larger than the actual value. The damage identification results subject to the above different d/γ for the three beam components were then treated using a 1D hybrid data fusion algorithm (analogous with Eq. (5a) to (5c), giving rise to optimal detection results as presented in Fig. 8(b) to (d), where the x axis corresponds to a bottom-to-top view of the beam components in Fig. 3(a) and (b). It can be seen that both the locations and sizes of the damaged zones can be clearly identified.

Conclusion

It was demonstrated in this study that the PE approach with its weak formulation can be effectively used to detect damage in one- and two-dimensional structural components without any prior knowledge of the baseline parameters of the structure under inspection. By assuming point-wise satisfaction of dynamic equilibrium conditions, the robustness of the PE approach can be enhanced in a statistical way. From the experimental results, it can be observed that, based on well-adjusted form and parameters of a weighting function and a hybrid data fusion algorithm, the method is able to reveal both the locations and sizes of damage with satisfactory accuracy and well-controlled measurement noise influence. A single vibration frequency was selected in the experiment for the construction of the damage indices. It can be anticipated that by using vibration displacements measured under an increased number of vibration frequencies, the detection accuracy can be further improved relying on data fusion algorithm. For the estimation of the baseline parameters, the errors are mainly attributed to measurement noise. Advanced signal processing technique should be adopted in further study aimed at increasing the accuracy of parameter estimation. Furthermore, besides 2D Gauss function, the effectiveness of other forms of weighting function is worthy to be explored in future work.

Acknowledgement

This work was supported by the National Science Foundation of China (No. 11602048) and the Fundamental Research Funds for the Central Universities (No. DUT16RC(3)060). This work was also supported by the National Science Foundation of China (No. 11772115)

Reference List

Aoki Y., Byon O. (2001) "Damage detection of CFRP pipes and shells by using localized flexibility method." Adv. Compos. Mater., 10, 189-198.

Cao M. S., Ostachowicz W., Bai R.B., Radzienski M. (2013) "Fractal mechanism for characterizing singularity of mode shape for damage detection." Appl. Phys. Lett., 103, 221906.

Fan W., Qiao P. (2011). "Vibration-based damage identification methods: a review and comparative study". Struct. Health Monit., 10(1), 83-111.

Farrar C.R., Doebling S.W. and Nix D.A. (2001). "Vibration-based structural damage identification". Philos. Transact. A Math. Phys. Eng. Sci., 359(1778), 131-149.

Gao D., Wang Y., Wu Z. Rahin G. and Bai S. (2014). "Design of a sensor network for structural health monitoring of a full-scale composite horizontal tail. Smart Mater." Struct., 23(5): 055011.

Gao D., Wu Z., Yang L. and Zheng Y. (2016). “Guide waves-based multi-damage identification using a local probability-based diagnostic imaging method.” Smart Mater. Struct., 25(4): 045009.

Giurgiutiu V., Rogers C.A. (1998) “Recent advancements in the electro-mechanical (E/M) impedance method for structural health monitoring and NDE.” Proceedings of SPIE on Smart Structures and Materials, 3329, 536-547.

Guo H.Y., Li Z.L. (2011) “A two-stage method for damage detection using frequency responses and statistical theory.” J. Vib. Control, 18(2), 191-200.

Ihn J.-B. and Chang F.-K. (2008). “Pitch-catch active sensing methods in structural health monitoring for aircraft structures.” Struct. Health Monit., 7, 5-19

Joshuva A. and Sugunaran V. (2017) “A comparative study of bayes classifiers for blade fault diagnosis in wind turbines through vibration signals.” Structural Durability $ Health Monitroing, 12(1) 69-90.

Kawiecki G. (2001) “Modal damping measurement for damage detection. Smart Mater. Struct.” 10, 466-471.

Kim J.T., Ryu Y.S., Cho H.M., Stubbs N. (2003) “Damage identification in beam-type structures: frequency-based method vs. mode-shape-based method.” Eng. Struct., 25, 57-67.

Lee Y.S., Chung M.J. (2000). “A study on crack detection using eigenfrequency test data.” Comput. Struct., 77, 327-342.

Liu K., Ma S., Wu Z., Zheng Y. Qu X. Wang Y. and Wu W. (2016). “A novel probability-based diagnostic imaging with weight compensation for damage localization using guided waves.” Struct. Health Monit., 15(2), 162-173.

Ostachowicz W., Kudela P., Malinowski P. and Wandowski T. (2009). “Damage localisation in plate-like structures based on PZT sensors.” Mech. Syst. Signal Pr., 23, 1805-1829

Pandey A.K., Biswas M., Samman M.M. (1991). “Damage detection from changes in curvature mode shapes.” J. Sound Vib., 145(2), 321-332.

Pandey A.K., Biswas M. (1994). “Damage detection in structures using changes in flexibility. ” J. Sound Vib. 169(1), 3-17.

Salawu O.S. (1997). “Detection of structural damage through changes in frequency: a review.” Eng. Struct., 19(9), 718-723.

Siddesha H and Manjunath N. H. (2017). “Structural damage detection in framed structures using under foundation settlement/rotation of bases.” Structural Durability & Health Monitoring, 12(1), 17-41.

Su Z., Ye L. and Lu Y. (2006). “Guided Lamb waves for identification of damage in composite structures: a review.” J. of Sound Vib., 295, 753-780

Wu Z., Liu K., Wang Y. and Zheng Y. (2015). “Validation and evaluation of damage identification using probability-based diagnostic imaging on a stiffened composite panel.” J. Intel. Mater. Syst. Str., 26(16), 2181-2195.

Xu H., Cheng L., Su Z., Guyader J.-L. (2011). “Identification of damage in structural components based on locally perturbed dynamic equilibrium.” J. Sound Vib., 330, 5963-5981.

Xu H., Cheng L., Su Z., Guyader J.-L. (2013). “Damage visualization based on local dynamic perturbation: theory and application to characterization of multi-damage in a plane structure.” J. Sound Vib., 332, 3438-3462.

Xu H., Cheng L., Su Z. and Guyader J.-L. (2015a). “A Pseudo-Excitation Approach for Damage Identification: From “Strong” to “Weak” Modality.” J. Sound Vib., (337), 181-198.

Xu H., Su Z. and Cao M.S. (2015b). “Dynamic perturbation characteristics for non-baseline structural damage diagnosis.” J. Vibroeng., 17(4), 1796-1804.

Xu H., Su Z, Cheng L. and Guyader J.-L. (2017) “On a Hybrid Use of Structural Vibration Signatures for Damage Identification: A Virtual Vibration Deflection (VVD) Method.” J. Vib. Control, 23(4), 615-631.

Yan A.M., Golinval J.C. (2005). “Structural damage localization by combining flexibility and stiffness methods.” Eng. Struct., 27, 1752-1761.

Zhao X., Gao H., Zhang G., Ayhan B., Yan F., Kwan C. and Rose J.L. (2007). “Active health monitoring of an aircraft wing with embedded piezoelectric sensor/actuator network: I, defect detection, localization and growth monitoring.” Smart Mater. Struct., 16, 1208-1217.

Figure 1. A schematic diagram of a plate structure containing a small damage zone

Figure 2. A flow chart for the damage detection procedure for two-dimensional structural components

Figure 3. (a) Front view of the plane structure, where the inspection regions on the plate and beam components are indicated by dashed red lines, and (b) back view of the plane structure, indicating the locations of the damage zones and excitation point

Figure 4. (a) Distribution of the measured vibration displacements within the inspection region on the plate component subject to vibration frequency of 1800 Hz, and (b) distribution of the damage index constructed using the original PE approach according to Eq. (1a) based on the vibration displacements

Figure 5. A two dimensional Gauss function within a square integration region Ξ , with a side length of $d = 10\sigma$

Figure 6. Distribution of the values of λ^* within the inspection region on the plate component of the plane structure, subject to $d / \gamma = 0.4$

Figure 7. Damage identification results constructed using Eq. (3a) based on estimated value of λ^* within the inspection region on the plate component, subject to (a) $d / \gamma = 0.3$, (b) $d / \gamma = 0.4$, (c) $d / \gamma = 0.5$ and $d / \gamma = 0.6$

Figure 8. Optimal damage identification results treated by data fusion algorithm for the (a) plate component, (b) beam I, (c) beam II and (d) beam III, as indicated in Fig. 3(a) and (b)

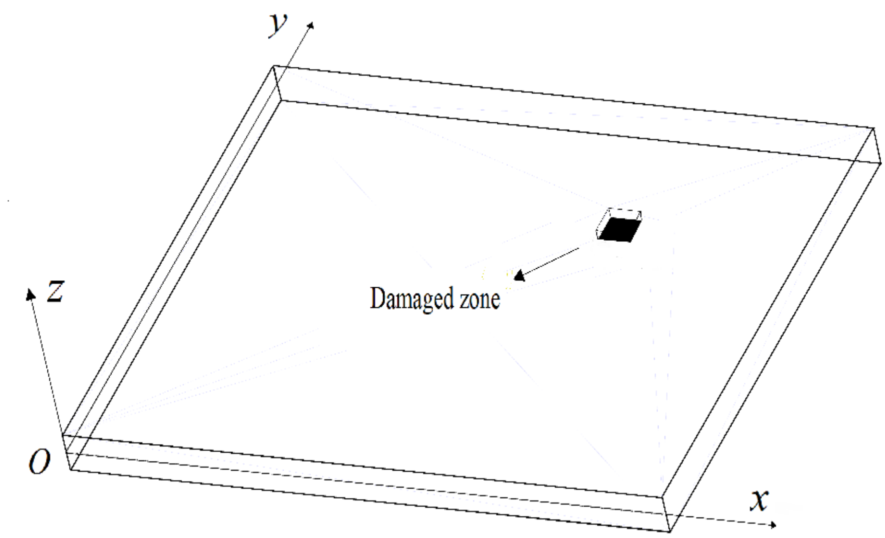

Figure 1

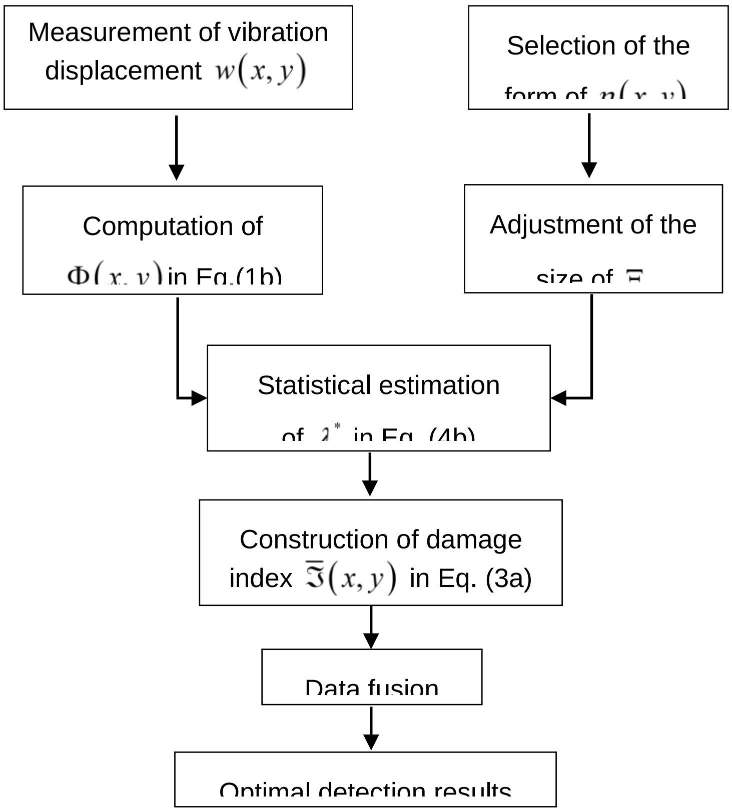
Measurement of vibration displacement $w(x,y)$
Selection of the form of $\eta(x,y)$
Computation of $\Phi(x,y)$ in Eq.(1b)
Adjustment of the size of Ξ
Statistical estimation of λ^* in Eq. (4b)
Construction of damage index $\overline{\Im}(x,y)$ in Eq. (3a)
Data fusion
Optimal detection results

Figure 2

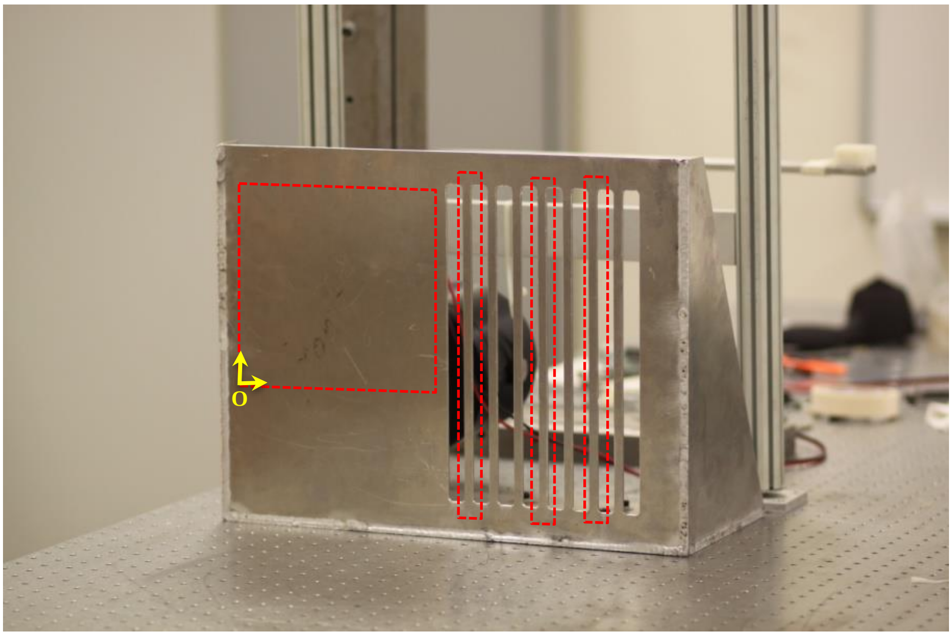

(a)

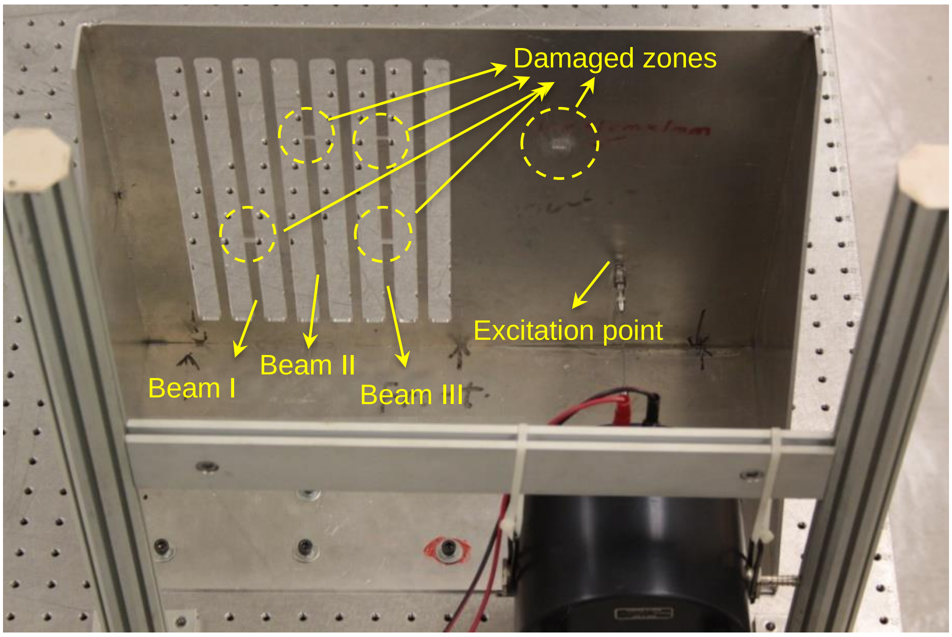

(b)

Figure 3

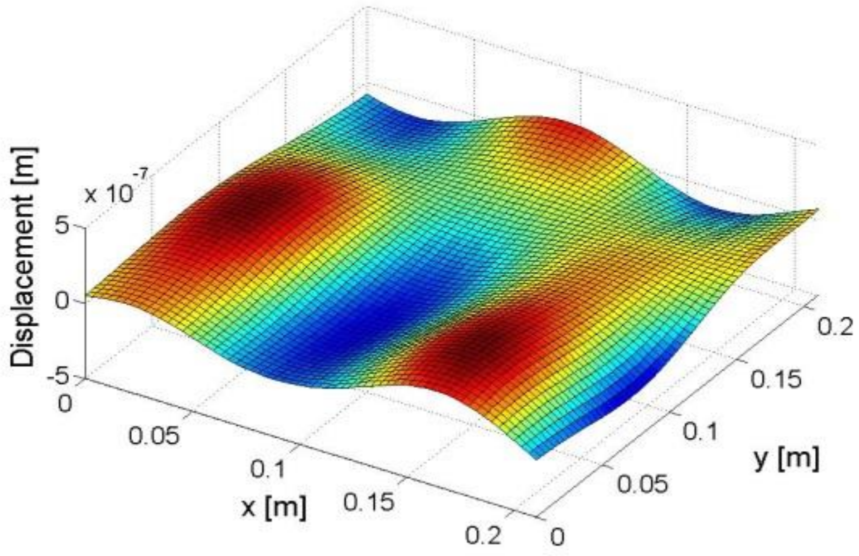
Displacement [m]
x 10^-7
5
0
-5
0
0.05
0.1
0.15
0.2
x [m]
0
0.05
0.1
0.15
0.2
y [m]

(a)

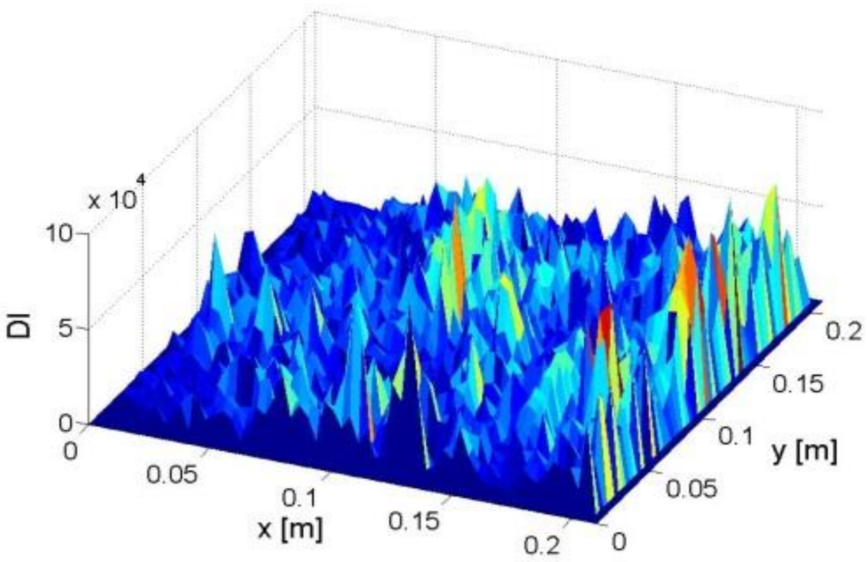
x 10^4
10
5
0
DI
0
0.05
0.1
0.15
0.2
x [m]
0
0.05
0.1
0.15
0.2
y [m]

(b)

Figure 4

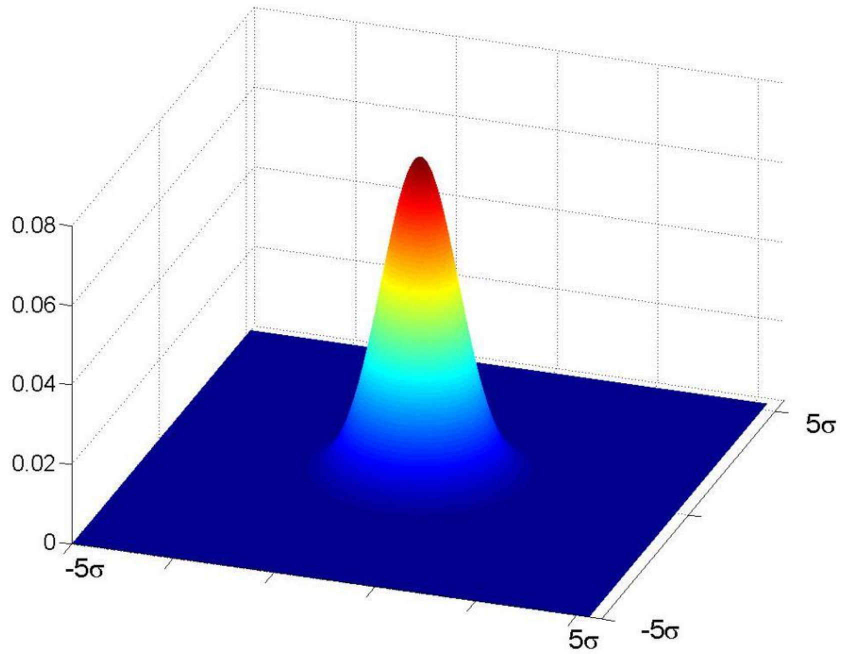

Figure 5

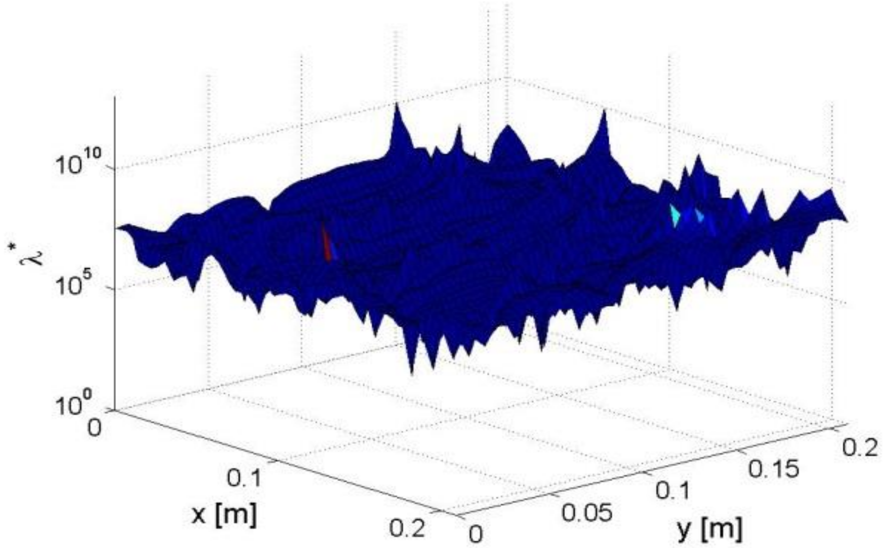

Figure 6

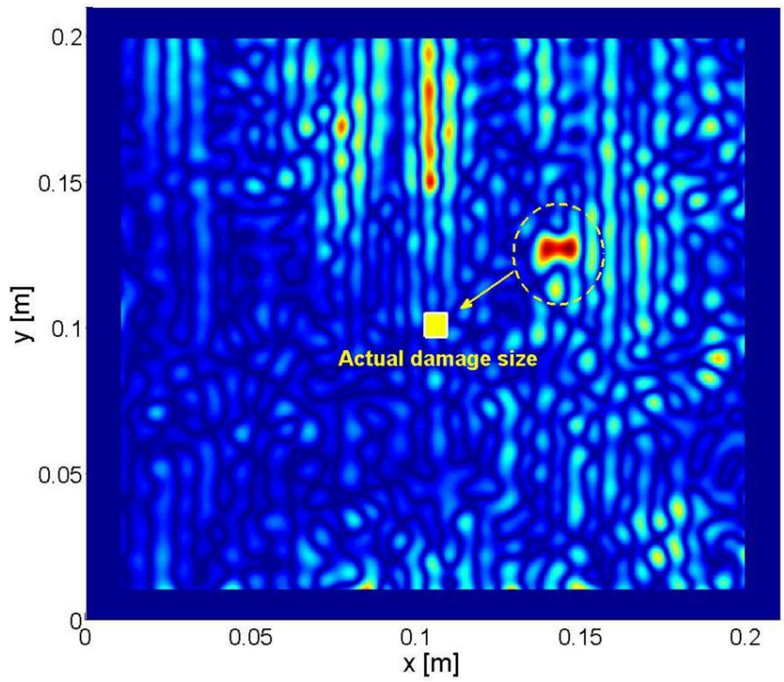
0.2
0.15
0.1
0.05
0
y [m]
0
0.05
0.1
0.15
0.2
x [m]
Actual damage size

(a)

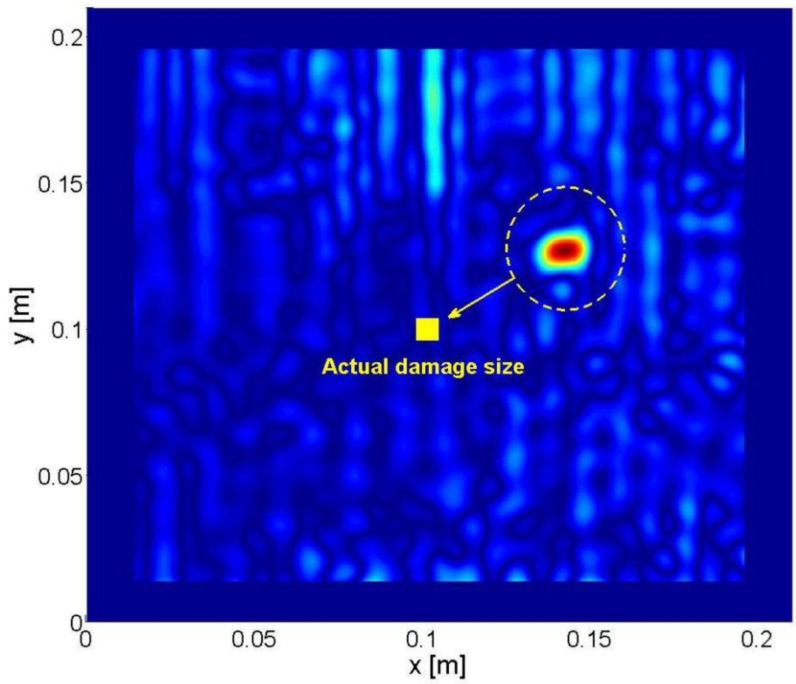
0.2
0.15
0.1
0.05
0
y [m]
0
0.05
0.1
0.15
0.2
x [m]
Actual damage size

(b)

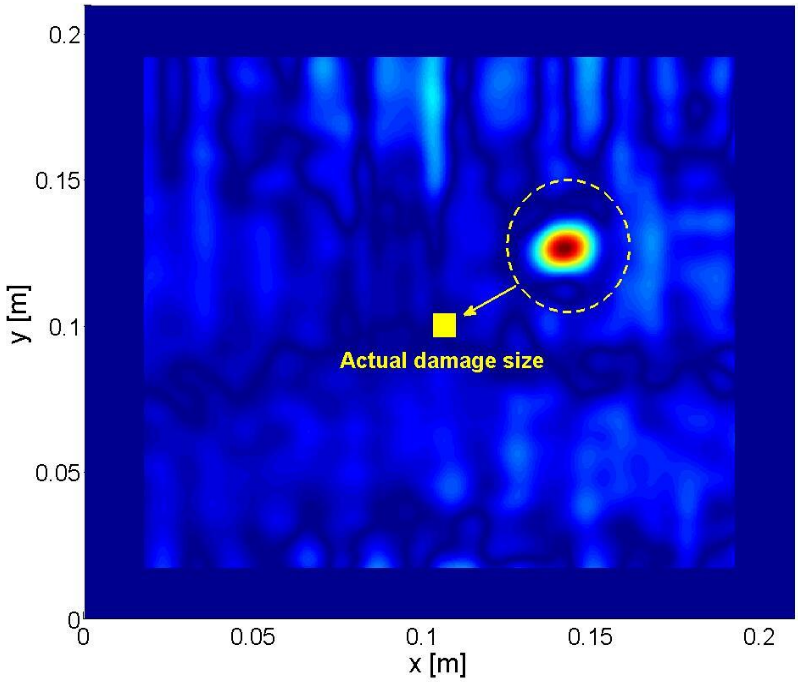
0.2
0.15
0.1
0.05
0
y [m]
Actual damage size
0
0.05
0.1
0.15
0.2
x [m]

(c)

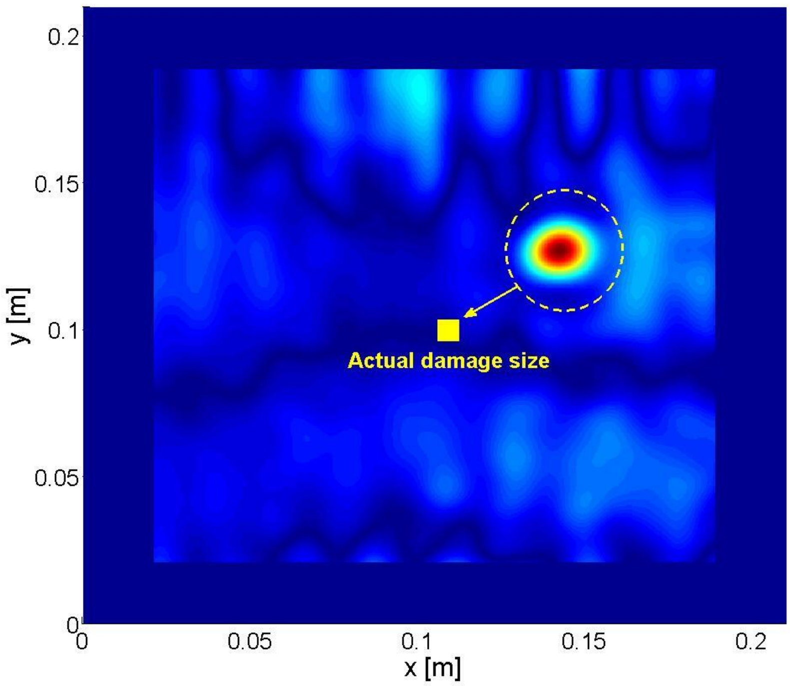
0.2
0.15
0.1
0.05
0
y [m]
Actual damage size
0
0.05
0.1
0.15
0.2
x [m]

(d)

Figure 7

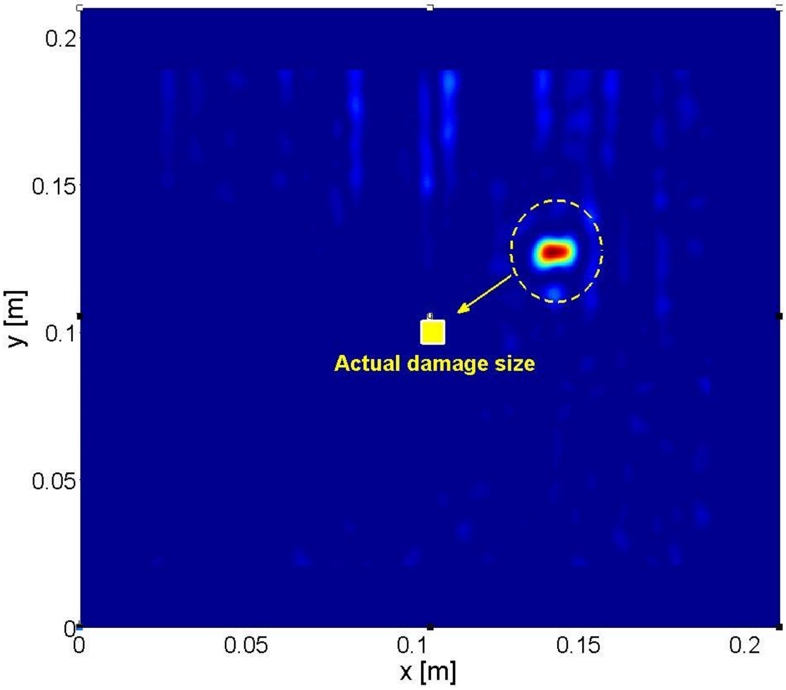

(a)

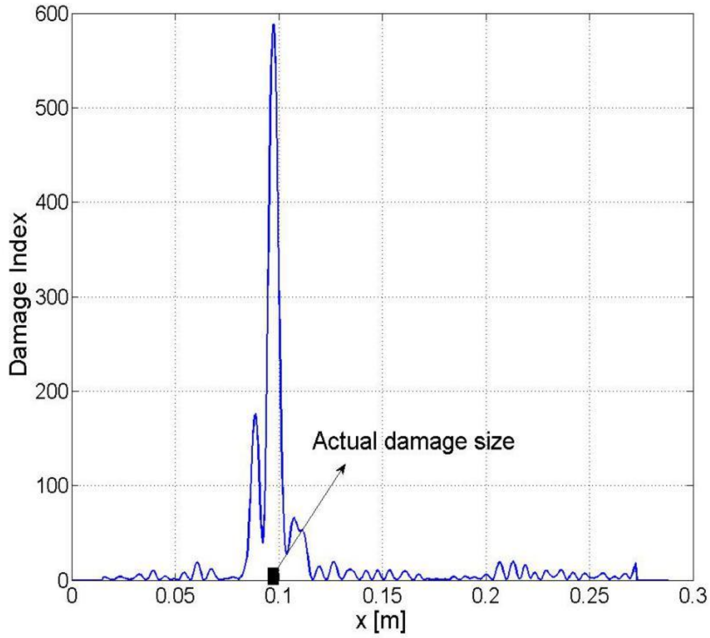

(b)

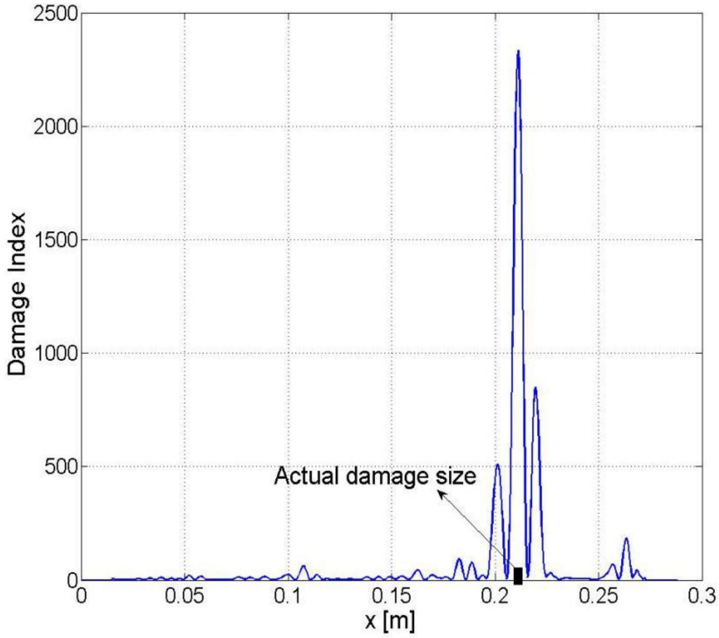
Damage Index
x [m]
Actual damage size
2500
2000
1500
1000
500
0
0
0.05
0.1
0.15
0.2
0.25
0.3

(c)

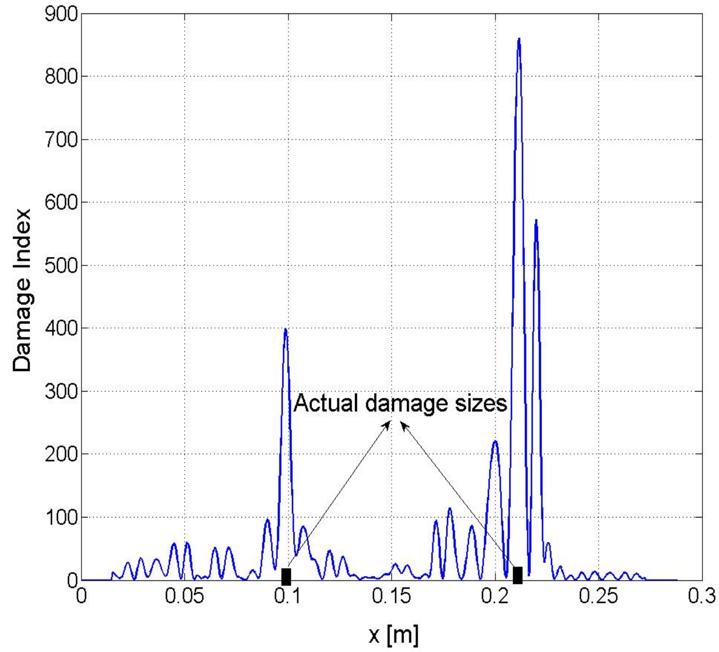
Damage Index
x [m]
Actual damage sizes
900
800
700
600
500
400
300
200
100
0
0
0.05
0.1
0.15
0.2
0.25
0.3

(d)

Figure 8